Available online at www.sciencedirect.com
SCIENCE DIRECT®
Nuclear Instruments and Methods in Physics Research A 515 (2003) 446–457
NUCLEAR INSTRUMENTS & METHODS IN PHYSICS RESEARCH Section A
www.elsevier.com/locate/nima

ATLAS MDT neutron sensitivity measurement and modeling

S. Ahlen[a], G. Hu[a], D. Osborne[a], A. Schulz[a], J. Shank[a], Q. Xu[b], B. Zhou[b,*]

[a] *Physics Department, Boston University, Boston, MA 02215, USA*
[b] *Physics Department, The University of Michigan, 500 E. University, Ann Arbor, MI 48109-1120, USA*

Received 6 August 2002; received in revised form 26 June 2003; accepted 29 June 2003

Abstract

The sensitivity of the ATLAS precision muon detector element, the Monitored Drift Tube (MDT), to fast neutrons has been measured using a 5.5 MeV Van de Graaff accelerator. The major mechanism of neutron-induced signals in the drift tubes is the elastic collisions between the neutrons and the gas nuclei. The recoil nuclei lose kinetic energy in the gas and produce the signals. By measuring the ATLAS drift tube neutron-induced signal rate and the total neutron flux, the MDT neutron signal sensitivities were determined for different drift gas mixtures and for different neutron beam energies. We also developed a sophisticated simulation model to calculate the neutron-induced signal rate and signal spectrum for ATLAS MDT operation configurations. The calculations agree with the measurements very well. This model can be used to calculate the neutron sensitivities for different gaseous detectors and for neutron energies above those available to this experiment.

PACS: 25.40.Dn; 29.40.Gx; 34.50.Bw

Keywords: Neutron sensitivity; Muon spectrometer; Energy loss and stopping power

1. Introduction

The measurement and modeling of the fast neutron sensitivity of the Monitored Drift Tubes (MDT) are critical R&D tasks for the ATLAS [1] Muon Spectrometer [2] electronics readout, trigger and shielding design. The issue is to understand the response of the primary precision muon detector element, the monitored drift tube, in the Large Hadron Collider (LHC) high-radiation environment. The main sources of the radiation background are very low-energy photons, neutrons, muons, and charged hadrons produced by interactions in the beam pipe wall, the forward-most calorimeters, the collimators, and the magnet quadrupole. The MDTs in the end-cap muon system will encounter a very high background of neutrons and photons. The expected rates from such background are estimated to be of order 10 kHz/cm^2.

In order to optimize the performance of the muon spectrometer, it is very important to gauge accurately the response of the MDTs in a high-radiation environment. For this purpose we conducted neutron test beam experiments using the neutron beam facility at the University of Massachusetts at Lowell [3] to make accurate

*Corresponding author. Tel.: +734-647-3760.
E-mail address: bzhou@umich.edu (B. Zhou).

0168-9002/$ - see front matter © 2003 Elsevier B.V. All rights reserved.
doi:10.1016/j.nima.2003.06.010

measurements of the MDTs' sensitivity to fast neutrons (neutron energy, $E_n > 100$ keV). The facility can produce well-calibrated mono-energetic neutrons with a relatively small portion of associated gamma radiation.

We exposed two ATLAS drift tubes (90 cm long and 3 cm diameter) to neutron beams in two different tests:

(1) The tubes were operated at a high voltage of 3270 V using a drift gas mixture of argon–carbon dioxide–nitrogen–methane (94:3:2:1) with 3 atm gas pressure.
(2) The tubes were operated at a high voltage of 3080 V using the standard ATLAS MDT gas mixture, argon–carbon dioxide (93:7), with 3 atm gas pressure.

The objectives of our study were to measure the MDT neutron signal sensitivities accurate to 10%, and to develop a simulation model to calculate the MDT neutron sensitivity to compare the predictions of the model to the measured data. In order to achieve the necessary measurement accuracy, a through study was made of the neutron facility radiation environment, particularly the photon background contamination.

This paper reports our test procedures adopted and the measurement results in details along with the features of simulation model and comparison of model predictions with measurements.

2. MDT neutron sensitivity measurement

2.1. Neutron beam facility

The facility at Lowell consists of a 5.5 MeV Van de Graaff proton accelerator. Protons bombard a thin metallic lithium target with tantalum backing to absorb residual protons. Neutrons are produced in a $^7Li(p,n)^7Be$ reaction with relatively small background gamma radiation. Using proton beams of different energies to hit the lithium target, one can obtain neutron beams with energies between 0.23 and 3.38 MeV. The neutron beam energy spread is very small (~ 50 keV) and has a flux of order $\sim 10^8$ n/s/sr in the beam direction.

Both the neutron energy and intensity decrease with increasing angle away from the forward direction. The angular dependence of neutron beam energy and neutron cross-section for a 0.5 MeV neutron beam are shown in Fig. 1. Fig. 1(a) shows the neutron–lithium differential cross section as a function of the neutron emission angle with respect to the beam forward direction; Fig. 1(b) gives the neutron energy as a function of the emission angle. In our experiment, the MDTs were irradiated by neutrons up to 60° away from the forward trajectory. The effects of this angular dependence were taken into account in the development of our simulation model.

It has been established by earlier experiments at Lowell that there are two kinds of gamma background sources in the neutron facility: (1) gammas from the beam line associated with the proton and lithium reactions; (2) gammas from the experiment hall due to the neutron absorption by the walls and other materials in the hall. We monitored the gamma background level in the test by using a gamma detector near the drift tube detectors. We found that the beam associated gammas can be reduced by more than 90% with a 2.54 cm lead block placed in front of the beam line. The level of the overall gamma background from the experiment hall was found to be small and isotropic.

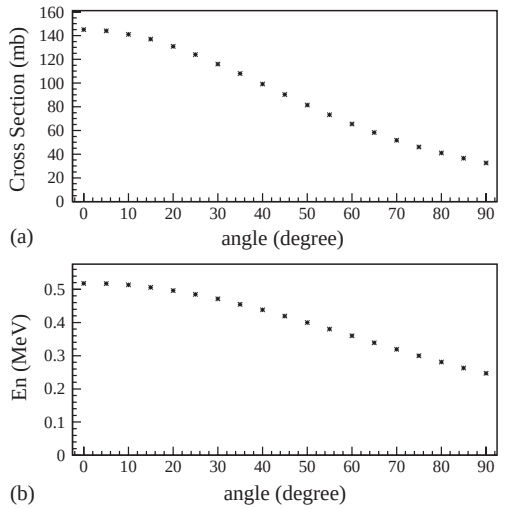

Fig. 1. Cross-section of neutron production and neutron energy as a function of neutron emission angle (in degrees) [4].

This gamma background was removed in the data analysis when separate measurements with the MDT located at different distances from the target were appropriately combined. This combination will be described in greater detail in the data analysis section.

In addition to providing neutron beams, the facility also provides a calibrated uranium fission chamber to the beam users to measure the neutron flux with a accuracy about 5%. The uranium chamber is a thin-walled aluminum cylindrical chamber, which has a radius of 6.35 cm, and thickness of 2.54 cm. Very thin layers of uranium are placed on the two inner surfaces of the chamber. Neutrons interact with the uranium atoms, and produce signals in the sensitive gas volume of the chamber.

2.2. The experiment

Fig. 2 is a diagram of the experimental setup used at the Lowell facility (not drawn to scale). The proton beam strikes the thin lithium target at the end of beam line. Neutrons from the target pass through a small uranium fission chamber a few centimeters from the target. The angles of coverage of the fission chamber are approximately $\pm 60^\circ$ with respect to the beam direction. Behind the fission chamber, there is a 2.54 cm lead barrier, so that beam-associated gamma radiation is highly attenuated. The test MDTs are located behind the lead shielding block. With the knowledge that the gamma background is uniform throughout the experiment hall, data taken with tubes at two different distances from the target can be assumed to have equal amounts of gamma background.

The signals from both ends of the tube are amplified using the electronics built for the L3 muon system [5]. Outputs from the amplifiers are sent to discriminators with thresholds set at 30 mV (corresponding to ~ 200 eV energy threshold based on ^{55}Fe calibration). Discriminator outputs are combined, in coincidence, to form a self-trigger for each tube. The trigger activates the LRS 9450 digital scope to record the drift tube signal waveforms and the output of a time–amplitude converter (TAC) (1 V = 5 ns) which provides data on the hit position along the tube. The digital scope data are stored on a computer using a General Processing Interface Board (GPIB). Signal rates from the proton beam and the uranium fission chamber, and from the MDTs are

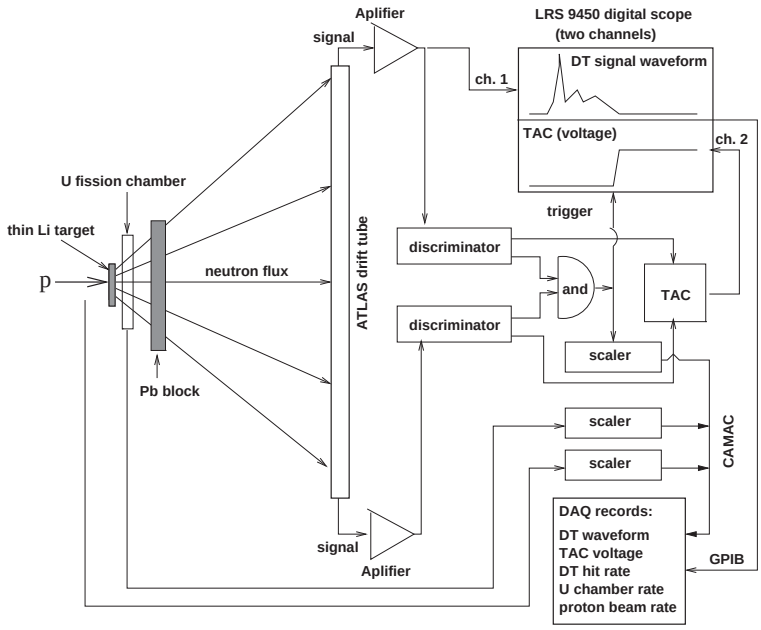

Fig. 2. Schematic of neutron test beam set up.

measured using CAMAC scalers. In addition, a two scintillator cosmic ray trigger was used to calibrate the drift tubes to cosmic rays before, during, and after the neutron exposure. The cosmic ray pulses were found to be typically greater than 100 mV. The shape of the waveforms that we observed from muons and neutrons interacting with the gas in the MDTs are actually quite different from one another as shown in Fig. 3. Neutron signals are more local, while muon waveforms are broad. Fig. 4 shows the MDT signal spectrum induced by a 0.5 MeV neutron beam. It was measured by integrating the waveforms of the neutron signals. Fig. 5 shows the recorded signal rates as a function of time for a typical test run. Fig. 6 shows a histogram of position of the event as measured by the time read from the TAC module. Since the center of the tube (45 cm from the tube end) has been calibrated to register 2.3 V, this diagram confirms our expectation that the majority of the signals are due to neutrons passing through the center of the tube, rather than by the gamma background illuminating the tube uniformly along its length.

2.3. MDT neutron sensitivity determination

We used the data that we obtained at Lowell to determine the sensitivities of the ATLAS MDTs to neutrons striking them. The sensitivity is determined by the expression

$$s = \frac{R_{\mathrm{n}}}{\langle F_{\mathrm{n}} \rangle \times \Omega_{\mathrm{MDT}} \times \eta} \tag{1}$$

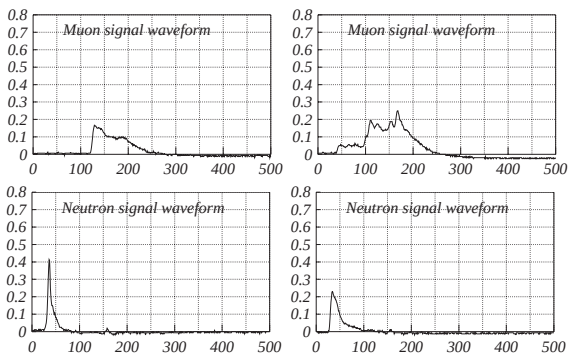

Fig. 3. Typical MDT waveform for muons and neutrons. The unit for the vertical axis is volt, and 2 ns for the horizontal axis.

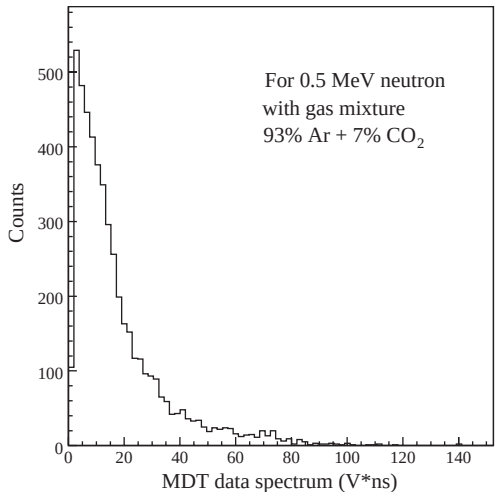

Fig. 4. Energy spectrum of the MDT from experimental data for test condition of 0.5 MeV neutron beam energy and using the standard ATLAS MDT gas mixture (93% Ar + 7% CO_2).

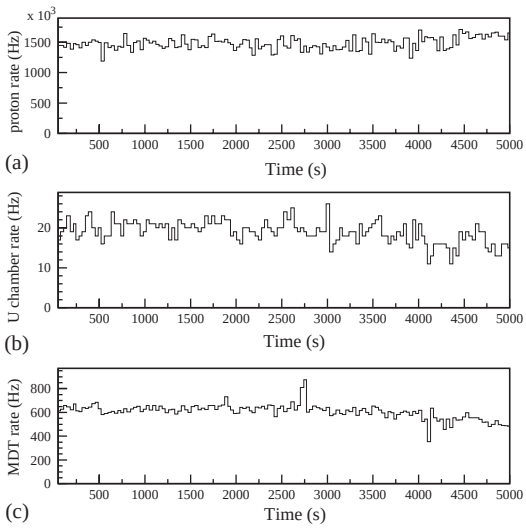

Fig. 5. The plot of proton beam rate (a), uranium chamber counting rate (b) and MDT tube counting rate (c) during one test run.

where s denotes the MDT neutron sensitivity, R_{n} is the neutron-induced signal rate in the MDT, $\langle F_{\mathrm{n}} \rangle$ is the average neutron flux, Ω_{MDT} is the detector solid angle coverage, and η is the neutron flux reduction constant mainly due to the lead barrier in front of the MDT. The calculations for determining each of these quantities are described in the sections below.

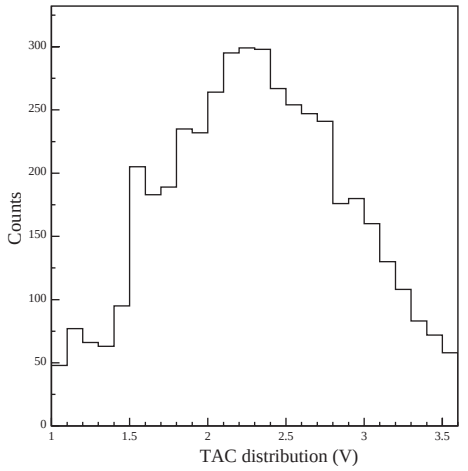

Fig. 6. The TAC (time–amplitude converter) signal distribution. It was recorded from the time difference between signals from the two ends of the tube (1 V = 5 ns), enabling one to localize the occurrence of the event in the tube.

2.3.1. Solid angle coverage

The solid angle coverage of a drift tube with length $2L$ and diameter D, located at a distance of d from the target, is calculated to be $\Omega_{\mathrm{MDT}} = 2DL/(d\sqrt{d^2+L^2})$, when $D \ll L$. The tube used in our test has the dimension of $2L = 90$ cm and $D = 3.0$ cm. As examples, the solid angle coverage of our test tube is 0.234 sr for a distance of 22.86 cm from the target, and 0.015 sr when the distance is 130.18 cm.

We must also calculate the uranium fission chamber coverages at the time of the chamber calibration and that during our tests to determine the neutron flux for different runs.

With the given cylindrical U chamber parameters (a radius of $r = 6.35$ cm and thickness of 2.54 cm) if it is placed at a distance d_{U} from the target, the solid angle is calculated to be $\Omega_{\mathrm{U}} = 2\pi(1.0 - d_{\mathrm{U}}/\sqrt{d_{\mathrm{U}}^2 + r^2})$. For $d_{\mathrm{U}} = 4.92$, 7.62 and 8.26 cm, the solid angle coverages are 2.4943, 1.46 and 1.30 sr, respectively.

2.3.2. Neutron flux

The average neutron flux ($\langle F_{\mathrm{n}} \rangle$) can be determined by the following formula:

$$\langle F_{\mathrm{n}} \rangle = \frac{R_{\mathrm{U}}}{\langle \varepsilon \rangle \times \Omega_{\mathrm{U}}} \tag{2}$$

where R_{U} is the uranium chamber signal rate, $\langle \varepsilon \rangle$ is the average U fission chamber efficiency corresponding to the fission chamber solid angle coverage (Ω_{U}) during the test.

We were provided the uranium chamber calibration data for a neutron energy of 0.5 MeV by the Lowell physicists:

$$\langle \varepsilon_0 \rangle \Omega_{\mathrm{cal}} = 3.33 \times 10^{-7} \tag{3}$$

where $\langle \varepsilon_0 \rangle$ is the average efficiency of the chamber, when $\Omega_{\mathrm{cal}} = 0.3224$ sr, which corresponds to the chamber calibration location at a distance of 19.05 cm from the target. Thus, the uranium chamber efficiency at calibration is: $\langle \varepsilon_0 \rangle = 1.03 \times 10^{-6}$. We need to make the corrections on the U chamber efficiencies since the U chamber solid angle coverage is different from the calibration in our test. We used the neutron beam energy angular dependence curve (Fig. 1) and the neutron–uranium cross-section to correct the U chamber efficiency. We found that the variations for all the test runs are less than 2%. For example, when the U chamber is located at a distance of 4.92 cm from the target, the corrected U chamber efficiency, $\langle \varepsilon \rangle$, is 1.048×10^{-6} compared to 1.03×10^{-6} given previously for $d_{\mathrm{U}} = 19.05$ cm.

2.3.3. MDT neutron-induced signal rate

The method we used to obtain the neutron-induced signal rate uses two separate sets of data, each taken at a different distance from the target, in order to remove the gamma background. Below we denote R_1 and R_2 to be the raw MDT signal rates for the MDT located at the first distance (d_1, corresponding to a solid angle Ω_1) and at a larger distance (d_2, corresponding to a solid angle Ω_2) from the target, respectively; R_γ to be the gamma-induced signal rate; and $R_{\mathrm{n}}(1)$ and $R_{\mathrm{n}}(2)$ to be the neutron-induced signal rates for two different distances. The recorded total signal rates induced in the MDTs can be expressed as

$$R_1 = R_\gamma + R_{\mathrm{n}}(1) \quad (\text{MDT at } d_1) \tag{4}$$

$$R_2 = R_\gamma + R_{\mathrm{n}}(2) \quad (\text{MDT at } d_2). \tag{5}$$

Therefore, elimination of R_γ term yields the following relation between the total raw signal

and the neutron signal rates:

$$R_1 - R_2 = R_n(1)\left(1 - \frac{R_n(2)}{R_n(1)}\right). \quad (6)$$

Since the neutron rate is proportional to the solid angle coverage times the neutron flux, this becomes

$$R_1 - R_2 = R_n(1)\left(1 - \frac{\Omega_2 \times \langle F_{n2} \rangle}{\Omega_1 \times \langle F_{n1} \rangle}\right) \quad (7)$$

which leads to the expression of the neutron-induced signal rate at the first distance:

$$R_n(1) = \frac{R_1 - R_2}{1 - (\Omega_2 \times \langle F_{n2} \rangle)/(\Omega_1 \times \langle F_{n1} \rangle)}. \quad (8)$$

2.3.4. Neutron flux reduction constant

The neutron flux was reduced in traversing the lead block used to suppress the beam-associated gamma radiation. In order to determine the flux reduction constant we used the Monte Carlo Ionization Chamber Analysis Package (MICAP) [6]. This calculation models the materials between the neutron beam and the MDTs, including the aluminum fission chamber, the 2.54 cm thick lead barrier, and the 0.4 mm aluminum tube wall through which the neutrons must pass before entering into sensitive gas area of the tube. The reduction constant depends on the neutron energy. The neutron beam energy profile as a function of neutron angle from the forward direction has been used in our simulation calculations. We found that the reduction of the neutron flux is approximately 40%. This implies that about 60% of the neutrons from the beam line actually reach the MDTs.

2.3.5. Results of the MDT neutron sensitivity

After having determined all the quantities expressed in Eq. (1), it is possible to determine the MDT neutron sensitivities for both MDT operation gas mixtures and voltages, as well as for different neutron beam energies.

Table 1 shows the test results for the MDTs using the argon–carbon dioxide–nitrogen–methane gas mixture (94:3:2:1) with operation voltage of 3270 V.

Table 1
Results of the neutron sensitivity measurement in our first test conducted in November 1997

Neutron energy (MeV)	0.5
U chamber distance (d_U) (cm)	4.92
U chamber counting (R_U) (Hz)	388
Neutron flux ($\langle F_n \rangle$) (Hz/sr)	1.57E + 8
MDT distance (d_1) (cm)	22.86
Tube signal rate (R_1) (Hz)	11.46E + 3
MDT distance (d_2) (cm)	130.18
Tube signal rate (R_2) (Hz)	1.73E + 3
Neutron signal ($R_n(1)$) (Hz)	10.39E + 3
Flux reduction constant (η)	0.67
MDT neutron sensitivity (s)	4.10E − 4

The MDTs used 3 atm pressure gas mixture of argon–carbon dioxide–nitrogen–methane (94:3:2:1) with operation voltage of 3270 V.

Table 2 shows the test results for the standard ATLAS Muon MDT gas mixture, argon–carbon dioxide (93:7) with operation voltage of 3080 V.

2.4. Uncertainties of the measurements

Based on the Eq. (1) that was used to obtain the neutron sensitivity of the MDTs we can express the uncertainty of the s measurement in the following equation:

$$\frac{\Delta s}{s} = \sqrt{\left(\frac{\Delta R_n}{R_n}\right)^2 + \left(\frac{\Delta \langle F_n \rangle}{\langle F_n \rangle}\right)^2 + \left(\frac{\Delta \eta}{\eta}\right)^2}. \quad (9)$$

The uncertainty in the neutron-induced signal rate (R_n) results from the variation of the proton beam current during each run. The determination of the R_n involves two sets of data, each of which has a different error associated with it. For example in our second test, for the 0.5 MeV neutron beam runs, the average tube counting rates (R_1) are 606, 583, 561 Hz, and R_2, 325 Hz. The associated standard deviations (σ_R) of these rates are 48.2, 27.1, 25.8 and 22.8 Hz, respectively. Therefore, the

Table 2
Results of the neutron sensitivity measurement in our second test conducted in August 1998

Neutron energy (MeV)		0.5		0.7
MDT distance (d_1) (cm)		50.8		50.8
Tube signal rate (R_1) (Hz)	6.06E+2	5.83E+2	5.61E+2	5.03E+2
U chamber distance (d_U) (cm)		7.26		7.26
U chamber rate (R_U) (Hz)	19.0	18.4	17.1	12.9
Neutron flux ($\langle F_n \rangle$) (Hz/sr)	12.7E+6	12.3E+6	11.4E+6	8.58E+6
MDT distance (d_2) (cm)		226.06		226.06
Tube signal rate (R_2) (Hz)		2.71E+2		3.10E+2
U chamber distance (d_U) (cm)		8.255		8.255
U chamber rate (R_U) (Hz)		11.8		9.70
Neutron flux ($\langle F_n \rangle$) (Hz/sr)		8.79E+6		7.23E+6
Neutron signal rate ($R_n(1)$) (Hz)	3.51E+2	3.28E+2	3.06E+2	2.82E+2
Flux reduction constant (η)		0.67		0.58
MDT neutron sensitivity (s)	5.56E−4	5.39E−4	5.40E−4	7.62E−4
Weighted Average sensitivity (s)		5.44E−4		7.62E−4

The MDTs used 3 atm pressure gas mixture of 93% Ar–7% CO_2 with operation voltage of 3080 V. At the neutron energy 0.5 MeV, there are three sets of data which correspond to three runs of the test.

relative error of the neutron-induced signal rate,

$$\frac{\Delta R_n}{R_n} = \sqrt{\left(\frac{\sigma_{R_1}}{R_1}\right)^2 + \left(\frac{\sigma_{R_2}}{R_2}\right)^2}$$

is in the range from 8.4% to 10.6%. For the 0.7 MeV neutron beam run, the uncertainty is 11.2%.

The error in the neutron flux measurement is estimated to be approximately 5% [7], including possible error in the uranium fission chamber acceptance.

Finally, the error in the η calculation using the MICAP program has an estimated error of approximately 5%. This is partially due to errors in the cross-sections used in the simulation, and partially due to the fact that we do not know precisely the components of the shielding materials.

The weighted error in the sensitivity measurements is determined to be 6.6% for 0.5 MeV neutron beam data after the three runs. The error for the 0.7 MeV neutron sensitivity measurement is about 13%.

3. Development of a simulation model

3.1. Introduction

Before preparing our computer simulation model, we made a simple calculation to estimate the order of magnitude of the MDT neutron sensitivity. The results of our simple estimate are close to what we measured in our experiments. We will describe the simple estimation in the next section.

Detail modeling of the MDT neutron sensitivity cannot be done by coding a GEANT [8] based simulation program as in most high-energy physics simulation tasks. We have to consider additional important factors in the simulation.

(1) The neutron transport code should use accurate cross-sections between the neutrons and the medium atoms. At low energies, the cross-sections are often not *smooth*. Such features should not be *averaged* in the simulation program, since they would lead to inaccurate prediction. Therefore, the usual hadronic tracking routine (GHEISHA) in GEANT cannot be used.

(2) Calculation of energy loss by ionizing particles to induce MDT electronic signals cannot simply use the *standard* Bethe–Bloch formula, since it applies to relativistic charged particles. Here, we are dealing with very low-energy nuclei recoiling from collisions with neutrons. In this energy regime (up to a few hundred keV), nuclear stopping power is significant. However, energy lost by this mechanism will not result in observable electronic signals. A more sophisticated model is required to simulate the electronic energy loss of the low-energy nuclear ions in the MDTs.

(3) The material description in the simulation program must be precise. In particular, the drift gas components cannot simply use an averaged atomic number and mass. Doing so will lead to inaccuracies.

We found that the MICAP [6] code in combination with the GEANT Monte Carlo simulation package is particularly well suited to our needs since it uses the GEANT framework to handle the detector geometry and material, but uses the *precise* measured cross-sections to simulate the interactions between the low-energy ($E<20$ MeV) recoil nuclei and the other atoms in the medium (very often, the cross-section curves are not 'smooth' as a function of energy). Therefore, we were able to use the output of this package (the recoil element atomic number Z and mass A, and the recoil energy) together with theoretical calculations by Lindhard et al. [9] to calculate the electronic energy loss of the low-energy recoil ions and thus to accurately reproduce the energy spectra and MDT sensitivities as a function of neutron energy.

3.2. Order of magnitude estimate

To estimate the probability that a neutron would interact with the gas atoms in the MDT, we need to calculate the mean collision length λ from the formula given below:

$$\lambda = \frac{1}{\sum_i N_i \sigma_i} \tag{10}$$

where σ_i is the cross-section of the neutron interacting with the ith atom in the drift gas, $N_i = (\rho_i/A_i)N_A$, with N_i, the number of atoms in one mol of gas, ρ_i, the density, and A_i, the atomic number of the ith atom. N_A represents Avagadro's constant in the expression.

Table 3
Data for each gas atom for standard ATLAS muon chamber gas mixture for 0.5 MeV neutron

Element	Ar	C	O
σ_i (b)	1.142	3.373	4.732
ρ_i (g/cc)	4.97×10^{-3}	1.13×10^{-4}	3.02×10^{-4}
A_i	40	12	16
N_i	7.48×10^{19}	5.68×10^{18}	1.14×10^{19}

The probability of an interaction between the neutron and the drift gas atoms is simply the average path length of neutrons in the MDT divided by the mean collision length λ.

With the information (shown in Table 3), the mean collision length (λ) for a 0.5 MeV neutron in the standard ATLAS MDT gas, is calculated to be $\lambda = 6329$ cm.

Assuming the average path length is approximately the diameter of the tube (3 cm), a good approximation in test beam conditions, we estimate the order of magnitude of the MDT sensitivity to 0.5 MeV neutrons is 4.75×10^{-4}, which is close to our experimental result of 5.44×10^{-4}.

3.3. MDT neutron sensitivity model

To model the MDT neutron sensitivity more accurately we developed a complete simulation program which includes the following major components:

(1) Neutron event generator—based on the neutron–lithium interaction angular distributions and differential cross-sections.
(2) Detailed test beam setup geometry description coded in the GEANT framework.
(3) Neutron transport code (MICAP) in the GEANT particle tracking framework to record the recoil element atomic number Z and mass A, and the recoil energy from neutron collisions with individual gas atoms.

(4) Use of low-velocity stopping power theory [9] to determine the electronic energy loss of the low-energy recoil ions inside a drift tube.
(5) Use of actual MDT signal threshold to calculate the electronic energy loss needed to record the simulated MDT signal.
(6) Determination the MDT neutron sensitivity based on the counts of neutrons entering the MDT gas volume, and the simulated MDT signal counts.

In the following sections, we first briefly describe the stopping power theory for low-energy nuclei and then briefly describe the neutron transport code (MICAP) used in our calculations. Following that we show our simulation results for comparison to data.

3.3.1. Theory of energy loss for low-energy nuclei

Neutrons are slowed down by nuclear collisions. These may be inelastic collisions, in which a nucleus is left in an excited state, or elastic collisions, in which the colliding nucleus acquires part of the energy of the neutron as kinetic energy. In either event, the nucleus loses all of the kinetic energy in the MDT gas. The rate at which it loses energy with respect to distance (dE/dx) is dependent on the gas through which it travels, and is often called the stopping power. At low energies, the total stopping power of the gas is divided between the electronic and the nuclear stopping power. Electronic stopping power is the amount of energy per unit distance that the recoil nucleus loses due to electronic excitation and ionization of the surrounding gas atoms. Nuclear stopping power is the energy loss per unit length that the nucleus loses due to collisions which transfer energy to motion of the gas atoms, but do not result in internal excitation. The proportion of electronic to nuclear stopping power depends on the recoil energy of the nucleus. If the recoil energy were very large, the nuclear stopping power would be very small compared to the electronic. However, in the energy range of the recoil gas atoms from neutron collisions, the nuclear stopping power plays a significant role in the energy loss of the recoil nucleus. A model by Lindhard et al. takes the nuclear stopping carefully into account.

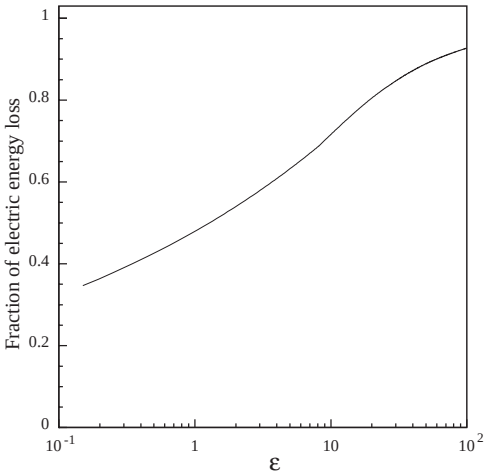

Fig. 7. Fraction of energy lost in electronic collisions as a function of the unit-less energy variable ε.

The theory is developed over a series of several papers entitled "Notes on Atomic Collisions." We have primarily used articles II and III of that series [10] in our calculations.

As has been verified by other experiments [11], we can use a graph of the electronic energy loss fraction as a function of recoil energy calculated by Lindhard et al. shown in Fig. 7. This curve uses a dimensionless variable (ε) that relates to the recoil energy (E_R):

$$\varepsilon = \frac{aA_2}{Z_1 Z_2 e^2 (A_1 + A_2)} E_R \tag{11}$$

where Z_1 = atomic number of the recoil nucleus, Z_2 = average atomic number of the medium. The parameter a is given by the following expression:

$$a = (0.8853) a_0 (Z_1^{2/3} + Z_2^{2/3})^{-1/2}. \tag{12}$$

where a_0 is the Bohr radius.

3.3.2. GEANT-MICAP Simulation program

The GEANT Monte Carlo simulation package is the most commonly used program to simulate particles interacting with detectors in detail. However, this simulation does not have the ability to track low-energy neutrons. In order to carry out simulations of these low-energy neutrons in the GEANT program, an interface to the low-energy neutron transport package (MICAP) has been

developed. The MICAP simulation specifically deals with tracking neutrons below 20 MeV. Interactions between neutrons with energy less than 20 MeV and nuclei are calculated all the way down to the thermal energy range (about 10^{-5} eV). The program uses cross-section data from the Evaluated Nuclear Data File (ENDF) [12]. The cross-section data include partial cross-sections, angular distributions of total and elastic cross-sections, and secondary energy distributions. The ENDF cross-section data is interpolated with an accuracy of 2%.

3.3.3. Results of the modeling

By combining the MICAP calculation of recoil energy of some gas nucleus with the theoretical curve taken from the stopping power theory, we are able to determine the amount of energy that has been lost due to electronic excitation and ionization of the atoms in the gas.

Fig. 8 shows the histograms of the frequency of events with each of the gas components, when $10^7 \times 0.5$ MeV neutrons were simulated for the test. Fig. 9 shows the gas atom recoil energy spectra for each of the elements. In these plots, the vertical scale is different for each graph. The simulated energy spectrum for the MDT signal when irradiated with 0.5 MeV neutron beams is presented in Fig. 10, which can be compared to the

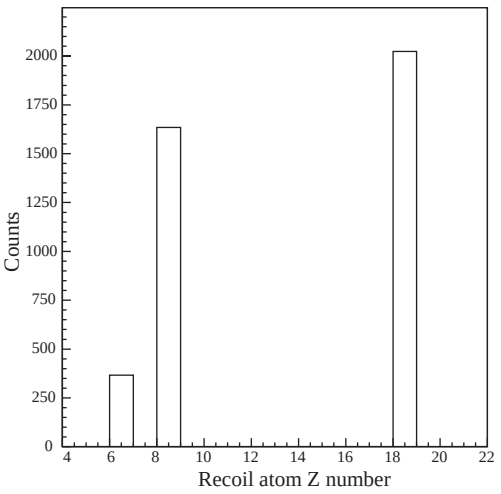

Fig. 8. Histogram of Z distribution of recoil nuclei.

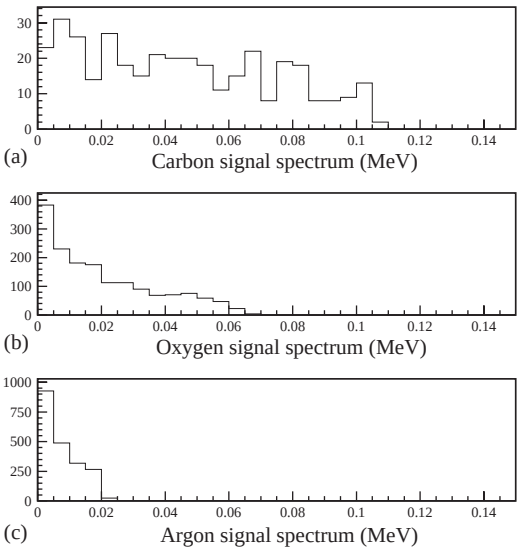

Fig. 9. Electronic signal spectra from each of the gas components. (a) For carbon; (b) For oxygen; and (c) For argon.

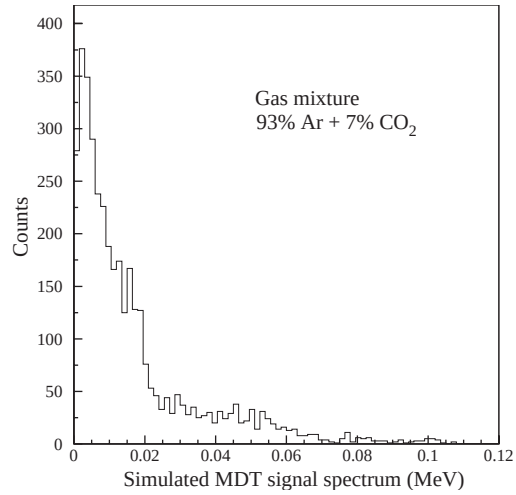

Fig. 10. Simulated energy spectrum of the MDT.

experimental spectrum (Fig. 4) to check the accuracy of our model. Figures shown in this section are for the standard ATLAS MDT gas mixture (93% Ar + 7% CO_2). The simulation results for 0.7 MeV neutron beams are similar.

The neutron sensitivity calculation results using our simulation model are listed in Table 4.

Table 4
Results of the neutron sensitivity calculation using the simulation model

Gas mixture	$Ar–CO_2–N_2–CH_4$ (94:3:2:1)	$Ar–CO_2$ (93:7)	
E_n (MeV)	0.5	0.5	0.7
s_{model}	4.05E − 4	5.75E − 4	6.23E − 4

The main sources of uncertainty in our model are the cross sections in the MICAP calculations and the stopping power treatment of electronic energy loss. The first one has an error of about 2% and the other is about 5–10%. There is also an uncertainty in the material content of the detector which must be input to the simulation program. For example, the gas proportions used in the simulation were not precise the same as the real gas mixture used in the test. Typical errors for each gas component in the gas mixture is about 5% (relative error). This could also contribute to the signal efficiency uncertainty in the calculations. By combining these sources, we estimate that the error in simulation is about 10%.

4. Conclusion

The goal of the ATLAS MDT neutron sensitivity studies was to use the Lowell neutron facility to experimentally determine the sensitivity of the MDT chamber to a beam of primarily monochromatic neutrons to an accuracy of about 10%, and to develop a sophisticated simulation model for calculations.

The results with the associated errors from the measurements and from the calculations are shown in Table 5, demonstrating that we have determined the ATLAS MDT neutron sensitivity by experiment and modeled it with Monte Carlo program.

From our results we can conclude that our simulation model could be used to study the responses of the gaseous detectors in high-radiation environment, such as the sensitivity of the ATLAS Muon MDT to background neutron radiation at energies beyond our test.

Table 5
Summary of the results for the ATLAS MDT neutron sensitivity studies

	Measured s	Calculated s
a	$(4.10 \pm 0.40) \times 10^{-4}$	$(4.05 \pm 0.41) \times 10^{-4}$
b	$(5.44 \pm 0.36) \times 10^{-4}$	$(5.75 \pm 0.58) \times 10^{-4}$
c	$(7.62 \pm 0.99) \times 10^{-4}$	$(6.23 \pm 0.62) \times 10^{-4}$

In the table, 'a' stands for the measurement condition of $E_n = 0.5$ MeV and gas mixture of $Ar–CO_2–N_2–CH_4$ (94:3:2:1); 'b', for $E_n = 0.5$ MeV and gas mixture of $Ar–CO_2$ (93:7); and 'c', for $E_n = 0.7$ MeV and gas mixture of $Ar–CO_2$ (93:7).

Acknowledgements

We would like to thank Dr. Gunter Kegel and Dr. David DeSimone for the great performance of the accelerator at Lowell and for the very valuable discussions with us about the neutron flux calculations. We thank Dr. Venetios Polychronakos suggesting us to use the Lowell neutron facility for the study. We would like to acknowledge J. Chapman's valuable comments on the manuscripts. We also thank Joel Goldstein and Jianguo Xu to help taking the test shifts.

References

[1] ATLAS Technical Proposal for a General Purpose pp Experiment at the Large Hadron Collider at CERN, CERN/LHCC/94-43, December 1994, The ATLAS Collaboration.
[2] ATLAS Muon Spectrometer Technical Design Report, CERN/LHCC/97-22, May 31, 1997.
[3] G.H.R. Kegel, et al., IEEE Trans. Nucl. Sci. 39 (6) (1992) 2052.
[4] H. Liskien, A. Paulsen, Atomic Data Nuclear Data Tables 15 (1) (1975) 57.
[5] The L3 experiment at LEP, CERN, an electronic note: "F/B-μ Chamber Frontend-Electronics".
[6] C. Zeitnitz, T.A. Gabriel, The GEANT-CALOR Interface User's Guide, Oakridge National Laboratory (August 1995); http://wwwinfo.cern.ch/asdoc/geant_html3/node352.html.
[7] Private communication with the Lowell Physicists, Dr. Gunter Kegel and Dr. David DeSimone. The U chamber used in the tests was provided by Kegel and DeSimone.

[8] R. Brun, et al., GEANT Version 3.21 (October 1994); CERN DD/EE/84-1 (September 1987), CERN Program Library Long Writeup W5013 (October 1994).
[9] J. Lindhard, M. Scharff, H.E. Schiott, K. Dan. Vidensk. Selsk., Mat.-Fys. Medd. 33 (1963) 14.
[10] J. Lindhard, V. Nielsen, M. Scharff, P.V. Thomsen, K. Dan. Vidensk. Selsk., Mat.-Fys. Medd. 33 (1963) 10 Guide, Oakridge National Laboratory (August 1995).
[11] G. Gerbier, et al., Phys. Rev. D 42 (9) (1990) 3211.
[12] Please see web site: http://www.nndc.bnl.gov/nndc/endf/.